International Journal of Refrigeration 150 (2023) 135–148

Contents lists available at ScienceDirect

International Journal of Refrigeration

journal homepage: www.elsevier.com/locate/ijrefrig

A 3-D FSI simulation for the performance prediction and valve dynamic analysis of a hermetic reciprocating compressor

Simulation FSI tridimensionnelle pour la prévision des performances et l'analyse dynamique des soupapes d'un compresseur alternatif hermétique

Aykut Bacak [a,b,*], Ali Pınarbaşı [a], Ahmet Selim Dalkılıç [a]

[a] Department of Mechanical Engineering, Faculty of Mechanical Engineering, Yildiz Technical University, 34349, Istanbul, Turkey
[b] Department of Thermodynamics and System Based Modelling, Research, and Development Center, Arçelik A.Ş. 34950, Istanbul, Turkey

ARTICLE INFO

Keywords:
Reciprocating compressor
Thermodynamic losses
pV indicator diagram
Reed valve motion
Fluid-solid interaction
Beam modeling

Mots clés:
Compresseur alternatif
Pertes thermodynamiques
Diagramme des indicateurs p-V
Mouvement des soupape à lamelles multiples
Interaction fluide-solide
Modélisation en faisceau

ABSTRACT

Hermetic reciprocating compressors consume the most electricity, and an improvement in compressor performance has a direct impact on compressor efficiency. Valve motion and pressure pulsation should be precisely predicted to assess the thermodynamic performance. In this paper, a three-dimensional fluid-structure interaction model validated by experiments is developed to investigate the oscillation motion of the suction and discharge reed valves, compression power, and mass flow rate of a hermetic reciprocating compressor operating under ASHRAE (54.4 °C/-23.3 °C) at the speed of 2100 rpm and additional specific refrigerator operating conditions such as (25 °C/-20 °C) and (40 °C/-25 °C) at the speeds of 1300 and 1600 rpms, respectively. Different from the others, no prior study has explored the whole compression cycle, including all four essential phases by showing the compressor's pV and valve oscillation diagrams under these operating conditions. In addition, the advanced mesh refinement method is computationally straightforward and has excellent numerical stability. Using this method as the third one in the literature, the mesh structure of complex geometries is generated without additional time or effort. Thus, the development of the model and the solution takes significantly less time than with other methods. When the obtained numerical outputs using the RNG k-ε turbulence model and experimental data are compared, the turbulence model is found to be reliable in the prediction of thermodynamic performance and valve lift. The deviations between experimental and numerical outcomes are 1.79%, -0.6%, and 3.44% for compression power and -1.28%, 0.6%, and 2.44% for mass flow rate regarding ASHRAE and additional operating conditions.

1. Introduction

In addition to the present energy crisis, the depletion of natural energy supplies has elevated the importance of energy efficiency. Due to these advancements, energy consumption requirements for energy-consuming equipment have gotten stricter. Studies on improving the energy efficiency of equipment such as the refrigerator compressor, which consumes the most energy, appear often in the scientific literature. In addition to experimental research, the continued development of computer-aided simulation software allows for the detailed creation of goods in a computer environment throughout product development procedures. These experimentally validated investigations also provide the discovery of subtleties that cannot be observed in the experimental setting. The fluid-solid interaction approach is used to examine hermetic reciprocating compressors with computer-aided software, as evidenced by the literature, due to the interaction of reed valve motions with the refrigerant and the compression and expansion processes of the refrigerant in the cylinder. Studies on the fluid-solid interaction approach have been published, primarily during the last decade, and are included

Abbreviations: AMR, Automatic mesh refinement; ASHRAE, American society of heating, refrigerating and air-conditioning engineers; BDC, Bottom dead center; CFD, Computational fluid dynamics; DEZ, Detrending extracting zooming; FSI, Fluid-structure interaction; LES, Large eddy simulation; PISO, Pressure-implicit with the splitting of operators; pV, Pressure-volume; RNG, Re-normalization group; rpm, Rotation per minute.

* Corresponding author.
E-mail address: aykut.bacak@arcelik.com (A. Bacak).

https://doi.org/10.1016/j.ijrefrig.2023.01.028
Received 1 November 2022; Received in revised form 28 January 2023; Accepted 29 January 2023
Available online 3 February 2023
0140-7007/© 2023 Elsevier Ltd and IIR. All rights reserved.

Nomenclature

C_m	Mass damping coefficient
E	Total internal energy
ε	Turbulence dissipation rate
F_P	Force due to pressure
F_O	Other forces
I	Turbulence intensity
k	Turbulence kinetic energy
K	Stiffness damping coefficient
k	Thermal conductivity
M	Mass
Q	Specific rate of heat generation
P	Pressure
ρ	Density
t	Time
T	Thermodynamic temperature
τ	Stress tensor
μ	Dynamic viscosity
V	Velocity
x	Distance
$\dot{x}$	Speed
$\ddot{x}$	Acceleration

below.

Jin et al. (2020) proposed the use of a detrending extracting zooming (DEZ) method to estimate the rotational speed of a compressor under laboratory conditions for a single-case scenario. In this study, the FSI model is developed, and the mechanism of pressure pulsation generation is investigated. The influence laws of pressure pulsation have been derived based on numerical simulations run at a variety of different operating speeds. It has been shown that the computation of rotational frequency is affected by the tendency element of pressure pulsation in addition to the harmonic apparatuses of such pulsations. Before separating the feature component of the pressure pulsation and improving the spectral resolution, the DEZ decreased the trend component of the pressure pulsation. This is accomplished without affecting real-time performance. The compressor speed decreases with a compression ratio below 2 s sampling time, and the maximum inaccuracy is ±1 rotation per minute (rpm). A novel DEZ-based speed measuring approach for hermetic reciprocating compressors first removes the component's pressure pulsation and lastly increases spectral resolution without sacrificing real-time performance.

To account for the unique motion of each valve plate, Zhao et al. (2018) developed a 3D computational fluid dynamics (CFD) model of a double-acting reciprocating compressor and proposed a mesh mapping approach. They look at how different turbulence models affect pressure pulsation. The thermodynamic performance can be reliably predicted by both turbulence models, even with small differences in the valve lift, as shown by a comparison of numerical models and real data. Pressure pulsation at frequencies below 500 Hz may be reliably predicted by the renormalization group (RNG) k-ε turbulence model, as shown by a fast Fourier transform (FFT) analysis. The detached eddy simulation (DES) model, operating at 420 rpm, can resolve frequencies more than 1500 Hz with a 10% margin of error. The DES model effectively predicts the valve lift fluctuation trend, even if the valve flow area is different from the experimental result.

Tao et al. (Tao et al., 2018) modeled a whole refrigerator compressor compression cycle. According to the analysis of the reed valve's motion, the frequency of the valve's oscillations has nothing to do with its rotating speed, which has grown proportionally with its increasing thickness. The FSI model is used to study how the rotation speed impacts the time it takes for the suction valve to close and the amount of backflow that occurs through the valve. This allows us to pinpoint the rotation speed at which the volumetric efficiency drops by 7% and the maximum amount of delayed closure is seen. Unlike the one-dimensional thermodynamic model, the FSI model can explore the delayed closing of the suction valve and backflow through the flow area.

Wu et al. (2022) used a three-dimensional fluid-structure interaction (FSI) model verified by tests using ADINA software to evaluate the oscillation motion of the piston-mounted valve. Air is the working fluid, and it is tuned to a low-speed compressible flow. The standard pressure interpolation method is utilized to simulate turbulence in the flow field using the RNG k-ε turbulence model. The lift integral of the valve on the piston is 4.5% less than that of the valve on the cylinder head, and the impact speed on the valve seat of the valve on the piston is less than that of the valve on the cylinder head, indicating that the suction valve installed on the piston is more dependable. Applying the equivalent inertia force to the reed valve simulates the single-acting compressor's suction operation and piston valve action.

Kawabata et al. (2022) studied the internal flow of the compressor using the three-dimensional FSI method and considering valve movements. To attenuate the pressure waves generated by the compressor, extra volumes are added in front of and behind the compression chamber, and the movement of the valve leaves is represented by beam components. Their analysis reveals that the mass damping coefficient and porosity of the reed valve must be taken into account to compare the movements of the reed valve to the experimental results. Test findings match the estimated internal pressure, and adjusting the damping factor C_m mimics the experiment's reed valve behavior. In addition to these, calculations are also affected by the porous material coefficient.

Hwang et al. (2017) examined the rigid body model and the 3D FSI model to establish the features of each valve model by examining the behavior of the discharge valve. For the R600a, the real gas model is utilized, and for the turbulence model, the realizable k–ε model with a standard wall function is employed. In addition, heat loss is not addressed for the compression chamber wall as insulation is anticipated. When the FSI model's valve closing condition is adjusted to account for extra displacement variations, this inaccuracy is decreased by more than 50%. Additionally, the FSI model with the added displacement fluctuations lowers the cooling capacity inaccuracy from 35% to 17%. Refrigerant overflow into the compression chamber during expansion causes several mistakes. Discharge valve displacement fluctuations cause backflow. The FSI model's valve closing condition is adjusted to account for displacement variations, reducing this inaccuracy.

González et al. (2017) analyzed and explained in detail a numerical method for taking into consideration the intertwined behavior of a reed valve and turbulent flow. Three-dimensional CFD analysis is used to examine the flow using large eddy simulation (LES) turbulence modeling and a hybrid of plate theory and the mode summation method. Lift amplitude and deformation fluctuations are found to be in good agreement between the model and experimental results when the Reynolds number is set to 10,000. Finally, a valve with a narrower gland is contrasted with one that has a wider one in terms of lift, pressure, force, and effective area. The findings indicate that the approach can provide an accurate representation of the flow field around the valve. However, a more comprehensive investigation of the effect between the reed and other bodies is required to address the valve lift inconsistencies.

Dynamics difficulties involving intense contact between a three-dimensional turbulent flow and plate-like structures are investigated by González et al. (2019). The method uses self-activated valves to model the linked flow mechanism. The numerical prediction will be used to examine the differences in efficiency between suction/discharge processes created with a straight and tapered exit port. Either choice

produces the same fluttering reed motion when the intake mass flow is held constant. To mitigate this pressure drop, a conical port is used. The approach simulates the linked flow process using self-activated valves. The purpose of the numerical prediction is to compare the performance of suction/discharge processes produced with straight and tapered exit port forms.

To replicate the unsteady flow dynamics and the motion of the fluttering valve in the cylinder, Coskun et al. (2016) developed a numerical flow model to emulate a fluttering suction valve in hermetic reciprocating compressors. A fully linked fluid-structure interaction (FSI) problem is addressed by using a restricted test geometry to illustrate the effects of the thickness, diameter of the circular component of the valve, and distance between the valve reed and the valve plate. Although the head diameter of the reed and the distance between the reed and the plate have minor effects on both the mass flow rate and displacement of the reed, increasing the thickness of the valve reed has a significant negative influence on the mass flow rate. The design characteristics of the valve reed have a significant impact on the mass flow rate together with the compressor's efficiency. Therefore, careful design of the reed valves is required to improve compressor performance.

Kim et al. (2006)investigated FSI simulation to solve valve dynamics considering heat transfer. Experiments are conducted to determine the properties of valve dynamics and to get the valves' dynamic behavior and pressure-volume diagram. The simulation of FSI is then done. Sequential quadratic programming is used to optimize the shape of a suction reed valve using a shape-optimization approach. The valve thickness is the most sensitive component to all reactions, including stress, volume, and deflection. Compared to the first design, the contact force is decreased by approximately 15% in the optimal design. Utilizing sequential quadratic programming and the form optimization approach, it is possible to determine the ideal design of a suction reed valve by calculating the efficiency factor, which is one of the most essential factors.

Choi et al. (2010) quantitatively investigated the steady-state characteristics of the linear compressor's valve system using the ADINA program, which accounts for FSI. The presumed fluid model is laminar flow. The working refrigerant is in the gaseous state, and the fluid flow is modeled as a low-speed compressible Navier-Stokes flow, which includes heat transfer. Sparse solver and the Newton technique of iteration scheme are utilized to address both a structural and a fluid issue, and an iterative solution approach is applied for the investigation of fluid flow with structural interactions. There is no correlation between the opening time of the discharge valve and the preload. When the pre-load is raised, the discharge valve closes more quickly.

Park et al. (2017) evaluated the suction valve for linear compressor cycle analysis using the FSI model and rigid body model. Unsteady fluid flow in three dimensions is explored. For turbulence, the realizable k-e model is used, whereas the real gas model is used for R600a. The rigid body model is used to mimic the behavior of the discharge valve, while the FSI model is utilized to simulate the behavior of the suction valve. Contrary to the experiment, the suction valve rigid body model opened twice while the FSI model opens three times. Nonetheless, the FSI model predicts the eventual closing time of the suction valve more accurately; the FSI model offers a more accurate forecast of refrigerant backflow after the bottom dead center (BDC). The rigid body model had a 4.1% EER error relative to the experiment, while the FSI model had 0.5%. This study's analytical models are not accounted for heat transfer through the cylinder wall or leakage through the piston clearance, resulting in a considerable disparity between the experimental cooling capacity and compression power findings and the EER results, which are in excellent agreement. Suction valve FSI models have lower EER errors than rigid body models.

Suction valve behavior is simulated using a three-dimensional model of a hermetic reciprocating compressor running on R600a under the American society of heating, refrigerating, and air-conditioning engineers (ASHRAE) operating conditions, which is explored by Lang et al. (2010). With the help of the semi-implicit method for pressure-linked equations-consistent (SIMPLEC) velocity and pressure coupling approach and the standard k-ε turbulence model, they can solve the fluid domain in 3D. The fluid solver is connected to the mechanical solver. Measurements taken with a laser doppler vibrometer are used to verify the accuracy of the corresponding numerical model. The primary impacts of the valve dynamics may be captured by this method with a high degree of precision and in a short amount of time, making it suitable for usage in industrial settings. Measured and simulated findings match well after validation. To demonstrate the method's capabilities, numerous main suction valve settings are changed and their impacts are analyzed using experimental and modeling approaches.

He et al. (2017) researched and experimentally validated a three-dimensional FSI model of the refrigerator compressor. The working fluid is R600A, and it is supposed to have a low-speed compressible flow operating at 0.68 MPa cylinder pressure and 0.067 MPa suction pressure. To simulate the turbulent flow in the valve and cylinder, the RNG k-ε turbulence model is used. Since the flow area of the suction valve expands as suction pressure increases, the instantaneous flow rate increases as suction pressure increases. Since the discharge valve flow area is relatively insufficient at the higher speed, the greater speed results in a higher pressure during the compression phase. The effect of polytropic exponent and density of refrigerant on the working process of the compressor is studied. The FSI model finds that operating conditions, rotation speed, and refrigerant affect cylinder pressure and compressor performance. Performance testing and compressor tuning may benefit from the FSI model.

Researchers González et al. (2017) looked at a three-dimensional CFD analysis using the LES turbulence model. The fluid is modeled using turbulence theory, while the solid is studied using a mixture of plate theory and the mode summation technique. The dynamically varying domains are addressed using lagrangian and arbitrary lagrangian-eulerian techniques for the solid and the fluid, respectively. The model and experimental data have good agreement in lift amplitude and deformation variations at a Reynolds number of 10,000. Finally, a case study comparing the outcomes of a valve with a narrower gland and one with a broader one is presented to illustrate the differences in lift, pressures, forces, and effective areas. This paper comprehensively describes a numerical methodology to account for the coupled behavior of a reed valve and a turbulent flow. The method is based on a partitioned semi-implicit scheme that only strongly couples the fluid pressure term to the structural solver. This work describes a numerical technique for reed valve-turbulent flow coupling. The partitioned semi-implicit methodology merges the fluid pressure term with the structural solver.

Tan et al. (2015) investigated the discharge valve movement in a rotary compressor using a three-dimensional FSI method. Since the discharge port is partially obscured by the cylinder and the roller, this special presentation also includes a second FSI model in which the discharge port is not obscured and the cylinder form is simplified to be cylindrical. The flow energy loss through the discharge valve is reduced by 68.8% compared to the FSI interaction model, while the impact velocity of the valve reed striking the retainer is increased by 2.9 m per second in the simplified model. The discharge port is partially obscured by the cylinder, indicating that the valve reed is slanted. The FSI model can accurately anticipate discharge valve movement and explore the discharge system. The valve reed tilts when the cylinder and roller partially cover the discharge port.

Kim et al. (2006) investigated a hermetic reciprocating compressor's heat transport and valve dynamics. To acquire the compressor's (pressure-volume) pV diagram, an encoder and pressure sensor are used. The experimental use of a strain gauge to examine the dynamic movement behavior of valves. In addition to heat transmission and structural valve dynamics, the effects of impact, oil stiction, and gas pulsation are taken into account in the simulations. Finally, shape optimization is done using the linear least square approach and sequential linear programming. Also, the highest possible price is paid for it. ADINA is used to

conduct a contact study based on the initial and optimized values of the suction reed valve. A 15% reduction in contact force is shown before using the optimal design. The thickness of the valve is the most sensitive part to all responses such as stress, volume, and deflection. The optimum value is obtained by using first, linear least square method and sequential linear programming, then shape optimization is implemented. With the initial and optimized value of the suction reed valve, contact analysis is performed using ADINA.

Single and dual muffler rotary compressors are studied by Chae and Kim (2010) to determine the effects of refrigerant flow on the discharge valve's motion and pressure fluctuations. To do this, it is used the FSI approach, employs numerical analysis to look at the flow field of the refrigerant and the behavior of the discharge valve. Consideration is given to the continuity, momentum, energy, and equation of state for the flow of the refrigerant, while the equation of structural dynamics is employed to describe the motion of the discharge valve. As the standard deviation of the pressure at the compressor, the output is reduced in the twin muffler scenario, and the energy spectrum values are typically smaller compared to the single muffler case, this may result in a lower noise level. Discharge valve displacement peaks with suction pressure peaks. Dual mufflers have a lower discharge valve displacement at the second peak than single mufflers and reduce refrigerant volume flow, lowering compressor efficiency and air conditioning capacity.

A three-dimensional CFD single-piston compressor system with dynamic intake and exhaust port flip valves is studied by Dhar et al. (2016). The mesh motion approach is used to replicate the intake port flip valve and the piston surface. Both of these components have swept volumes that intersect with one another and may interact with one another when the compressor is in operation. Using a powerful ODE solver and the pressure distribution that is operating on the valve, the FSI program estimates the motion of the valve. Flow rates during the discharge show a significant jump, but flow rates during the suction imply a more even distribution throughout the suction stroke. When the dynamics suggest that the valves are entirely closed, the simulation can manage the complete closure of the valves while leaving nearly no space between the valves and their seats. The present flip valve dynamics provide correct pressure distribution on valve surfaces, which improves valve motion prediction, compressor performance, and efficiency prediction. Template-based meshing and flow solver robustness make simulation straightforward and rapid. This innovative model is beneficial for designing and analyzing reciprocating single-piston compressor systems because of its ease of use, short simulation turn-around time, and important information from transient 3D simulations.

Rowinski et al. (2018) designed a small displacement refrigeration compressor with an automated grid. The FSI between deforming reed valves and flow is modeled using a two-way coupled technique. The fluid is solved using finite volume, whereas the solid uses finite elements. The model is verified using observed mass flow rate, pressure, temperature, and valve lift for R-404a and R-449a. While a coarse grid can forecast power, mass flow rate, and pressure oscillation frequency, a finer mesh is needed within the cylinder and discharge muffler to predict pressure amplitude. The findings demonstrate that grid discretization is more essential than temporal discretization when operating with a time step restricted by sound and local fluid velocity. The beam and leakage model with thermal boundary conditions along the discharge flow route can be improved.

Pham et al. (2018) created a three-dimensional CFD model of a scroll compressor employing circling scrolls and deforming reed valves. An FSI model is used to calculate the motion of the discharge reed valve. This model takes into account the geometry of the valve as well as its many cross-sections. There is low numerical diffusion, high numerical accuracy and stability of the orthogonal cells, and reasonable validation of the experimental compressor that is measured. It is simple to make changes to the geometry, and it is simple to incorporate complex moving boundaries like the orbiting scroll and the reed valve. Additionally, there is reasonable validation of the experimental compressor that is measured. For engineering design optimization, these are only some of the considerable advantages that may be gained by using the technique. Other advantages include a rapid transformation from CAD geometry to a CFD model, the simplicity of making modifications to the geometry, and the convenience with which complicated moving boundaries may be included. The method has high numerical convergency and stability of the orthogonal cells, and reasonable validation with the experimental data.

Hopfgartner et al. (2017) studied a suction valve closed by an electromagnetic coil in the muffler's neck. Before the piston hits BDC, voltage is supplied to the coil, creating a magnetic force that closes the valve. By reducing the reed valve's preload, the flow resistance through the valve is loaded. Numerical simulations for ASHRAE cycle (-23 °C/55 °C) operating conditions reveal 0.68% lower power usage. Reversed mass flow via the suction port rises from 0.26 to 1.6%, reducing total mass flow by 0.31%. Measurements validated modeling findings (decreased power consumption by 0.71%, cooling capacity by 0.32%) and indicated an enhanced COP of 0.39%. In a second working state, the COP is 1.72% higher. The electromagnetic coil-adapted suction valve improves compressor performance. This suction valve should be under control by a proper automation solution since the operation circumstances vary continuously.

The small displacement refrigeration compressor is modeled by Rowinski et al. (2016) using the cartesian cut-cell finite volume approach. This study focuses on a hermetic refrigeration compressor with a displacement of 13.1 cm^3 that uses R134a as its refrigerant. It is going to proceed with the assumption that there will be a low back pressure (LBP) and that the condensing temperature will be 54 °C. The compressor has a normal working speed of 3000 rpm. Monitors are placed on the cylinder to keep an eye on the pressure as well as the suction and discharge reed lifts. The amount of numerical uncertainty is rather low when compared to the experiment for pressure and valve lift. The model is more accurate than the experiment. Compared to the pressure and valve lift measurements, the model's numerical uncertainties are minimal. This shows two things: First, this work's numerical method shows numerical accuracy throughout the range of values examined. Second, physical models have higher uncertainty than numeric ones. Realistic leakage and stiction models add crucial physics to the cartesian cut-cell finite volume approach.

The performance of a hermetic reciprocating compressor is analyzed by Lang et al. (2010) using the CFD technique. They considered both ideal and actual gas approaches to the refrigerant when conducting their analysis. In every simulation that has been run, valves have been modeled as sliding flat plates that are parallel to one another. In this part of the experiment, actual and ideal gas assumptions, as well as the results of the experiment, are compared and contrasted. When using the equation of state for an ideal gas, the amount of divergence from the behavior of a real gas is insignificant. They stated that having accurate boundary conditions for the walls of the cylinder, as well as the suction and discharge line, is more important than having a well-augmented gas model. The difference between the ideal gas and the real gas is only about 1.3% when the two sets of results are compared. The mass flow rate through the comparable system, which is directly proportional to its cooling capacity, also differs by only about 0.46%. The ideal gas equation of state shows small deviations from actual gas behavior. Industrial users value significantly decreased computation times above modestly increased accuracy. Real gas models destabilize simulations, resulting in non-converged results.

In this study, numerical investigation methodology is given to validate hermetic reciprocating compressors under ASHRAE and specific refrigerator operating conditions such as (25 °C/-20 °C) and (40 °C/-25 °C). However, no prior study has explored the whole compression cycle, including all four essential phases by showing the compressor's pV and valve oscillation diagrams. In this study, a three-dimensional FSI model is conducted to simulate the entire operation of a hermetic refrigerator compressor, and obtained numerical outputs are compared

with experimental ones. This research identifies the oscillation features of suction and discharge reed valves based on the suggested FSI model and investigates the effects of the various operating conditions and differences in reed valve motions regarding the operating condition by using the Advanced Mesh Refinement method. In this method, an orthogonal basis grid of the user's selection fills the fluid domains. At the points where the triangulated surface meets the base grid, the cells of the grid are divided into polyhedral with arbitrary sides. This means that for every given size of the underlying grid, the volume represented by the cut cells is always the same as the volume of the original triangulated surface. Since the mesh is formed without any user input, it can readily account for complicated boundary forms and movements. The technique is computationally straightforward and has excellent numerical stability since it is based on regular orthogonal grids. Using this method as the third one in the literature apart from Kawabata et al., (2022) and Rowinski et al. (2018) on this subject, the mesh structure of complex geometries is generated without additional time or effort. Thus, the development of the model and the solution takes significantly less time than with other methods. Moreover, since the performance of the compressor varies with the operating condition, it is important to analyze cooling capacity, and compression power metrics at various operating conditions as performed in this investigation. Consequently, the findings of this study are expected to be evaluated as useful for researchers who are interested in determining the performance losses of hermetic reciprocating compressors in a variety of operational settings.

2. Experimental method

The FSI model is validated using an experiment that measured the pV diagram, the suction, discharge, and cylinder pressure values versus crank angle, and the suction and discharge valve displacement. An existing refrigerator compressor is modified to allow for the installation of sensors, as indicated in Fig. 1 since the research concerned the pressure for suction, discharge, and cylinder, and the displacement of suction and discharge valves. Due to the compact size of the refrigerator compressor, capturing the pV diagram in the experimental investigation is a difficult task. The transient pressure history is measured using high-precision pressure sensors (Kulite, XT-190(M)) with a sampling rate of 50 kHz and a measurement accuracy of 0.1%. The sensors are fitted with attention to the compressor's size and real construction. As seen in Fig. 1, the sensor for measuring the pressure in the suction, discharge, and the cylinder is integrated with the suction plenum, cylinder cover, and valve seat to have the smallest impact on the flow structure. The simultaneous bridge module is used to acquire strain signals from the quarter bridge using the strain gauge with a measurement precision of 1.0%. Table 1 outlines the structural parameters that the compressor must meet to function properly.

Table 1
Specifications of an investigated compressor.

Design Parameter	Value
Cylinder bore	24.28 mm
Crankshaft diameter	10.64 mm
Eccentricity	2.75 mm
Connection rod length	38.7 mm
Oil viscosity	10 cSt
Reed valve thickness	0.2 mm

3. Numerical methods

Refrigerator compressors function by coordinating the flow of refrigerant with the movement of the reed valve. Under pressure, the reed valve bends, altering the flow of the refrigerant. Consequently, the simulation of refrigerator compressors requires the solution of structural and hydrodynamic governing equations and consideration of their interconnections. This study offers a 3D FSI model using CONVERGE 3.0 to investigate compressor operation under specified operating conditions given in Table 2 by specifying boundary conditions as described in Table 3. This FSI investigation divided the compressor model into fluid and structural domains.

There is a model based on the crank-angle diagram within the CONVERGE software, including parameters for connecting rod length, piston diameter, and eccentricity. During the modeling phase, the geometry of the piston begins at the piston's bottom dead point (180°) and completes its movement again bottom dead point (540°). The flow and heat transfer solutions of the compressor are found in line with the calculation of the crank angle diagram by moving the piston between the lower and higher dead centers and computing the corresponding equations. In this software, there are two FSI models for modeling the reed valve: beam and rigid. In addition to defining the thickness, width, density, and elasticity modulus of the valve, the origin, direction, and normal of the reed valve are also defined, allowing for the study of the reed valve.

3.1. Fluid domains

According to Fig. 2, the suction, cylinder, discharge, and discharge pipe regions are the components that made up the fluid domain of the model of the compressor.

The laws of classical mechanics and thermodynamics guided the motion of a continuous refrigerant fluid domain inside the compressor model. These concepts are in place to ensure that the model is accurate. As illustrated in the equations, they are capable of being stated in conservative forms of mass, momentum, and energy. (1)–(4)

Continuity equation:

$$\frac{\partial \rho}{\partial t} + \nabla\left(\rho \vec{V}\right) = 0 \tag{1}$$

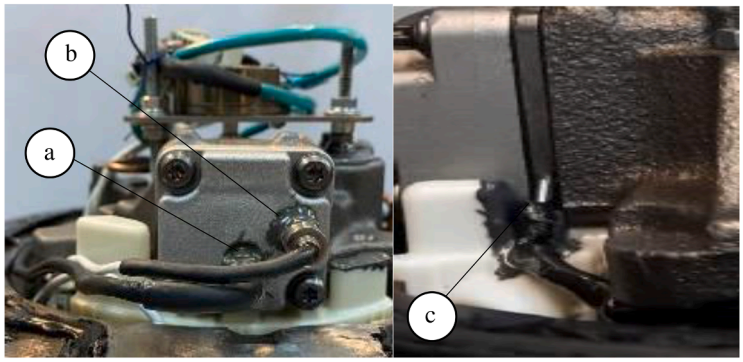


Fig. 1. The installation of the pressure sensor (a) suction pressure, (b) discharge pressure, (c) cylinder pressure.

Table 2
Operating conditions.

Operating Condition	Evaporation Temperature [°C]	Condensation Temperature [°C]	Evaporation Pressure [bar]	Condensation Pressure [Bar]	Compressor Speed [rpm]
ASHRAE (54.4 °C/−23.3 °C)	-23.3	54.4	0.624	7.61	2100
(25 °C/−20 °C)	-20	25	0.725	3.507	1300
(40 °C/−25 °C)	-25	40	0.584	3.512	1600

Table 3
Boundary conditions.

Component	Momentum boundary condition
Inflow	Pressure inlet, constant total pressure
Suction plenum	Stationary, Law-of-the-wall
Inlet pipe wall	Stationary, Law-of-the-wall
Suction muffler wide wall	Stationary, Law-of-the-wall
Suction muffler inner wall	Stationary, Law-of-the-wall
Suction muffler long wall	Stationary, Law-of-the-wall
Cylinder wall	Stationary, Law-of-the-wall
Piston wall	Motion through crank-slider mechanism at measured frequency
Discharge pipe wall	Stationary, Law-of-the-wall
Discharge muffler wall	Stationary, Law-of-the-wall
Outlet pipe wall	Stationary, Law-of-the-wall
Outflow	Pressure outlet, constant total pressure
Cylinder cover	Stationary, Law-of-the-wall
Suction reed valve	Deforming through beam model, Law-of-the-wall
Discharge reed valve	Deforming through beam model, Law-of-the-wall

Momentum equation:

$$\rho\left(\frac{\partial \vec{V}}{\partial t}+\left(\nabla \vec{V}\,\vec{V}\right)\right)=-\nabla p+\nabla\tau \tag{2}$$

The stress tensor is given by:

$$\tau=\mu\left[\nabla \vec{V}+\left(\nabla \vec{V}\right)^{T}\right]-\frac{2}{3}\vec{V}I \tag{3}$$

Energy equation:

$$\frac{\partial}{\partial t}\left[\rho\left(E+\frac{1}{2}V^{2}\right)\right]+\nabla.\left[\rho V\left(E+\frac{1}{2}V^{2}\right)\right]=\nabla.(k\nabla T)+\nabla.(-pV+\tau.V)+Q \tag{4}$$

where ρ is the density, t is the time, V is the velocity vector, τ is the stress tensor of the fluid, E is the total internal energy, k is the thermal conductivity of the fluid, T is the thermodynamic temperature, Q is the specific rate of heat generation.

Using the Redlich–Kwong model (Redlich and Kwong, 1949), the working fluid considered to be a low-speed compressible flow is R600A assumed as a real gas. This flow is assumed to be compressible. The RNG k-ε turbulence model is used to simulate the turbulent flow in the fluid domain under specific operating conditions. The conventional pressure interpolation technique is chosen, and the pressure-implicit with the splitting of operators (PISO) approach is utilized to address the pressure-velocity coupling issue. Both of these schemes are used in conjunction with the fluid domain. Through the use of a cut-cell method implemented with adaptive mesh refinement of the element, the fluid domain is discredited. At the beginning of the simulation, the top of the piston is modeled as a moving wall in the fluid domain, and it is assumed that it would travel from the top dead center (TDC) to the BDC.

The finite-volume approach is used to solve the continuity, momentum, and energy equations. The core of the computational cells is

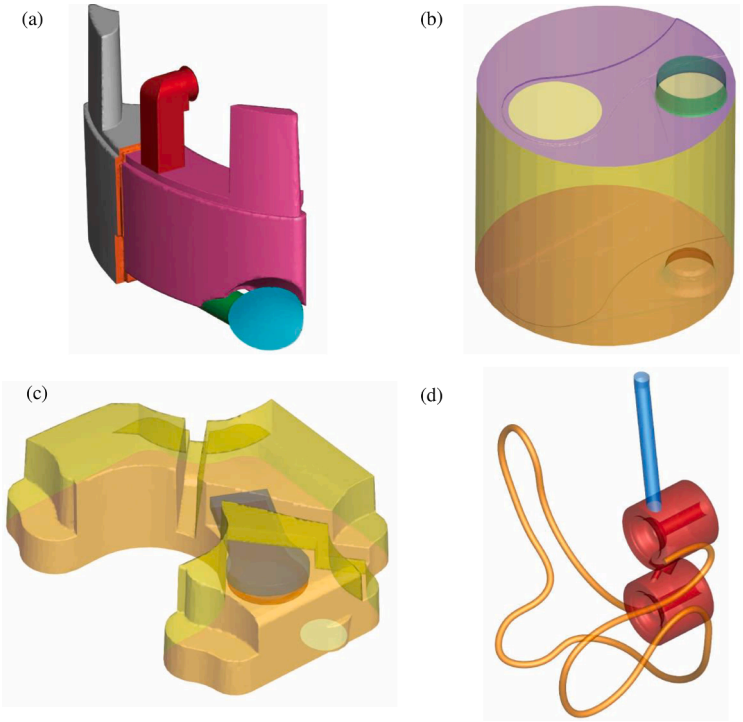


Fig. 2. The domain of the regions of hermetic reciprocating compressor, (a) suction, (b) cylinder, (c) discharge, and (d) discharge pipe, respectively.

where all model values are compiled. The algorithm developed by Rhie and Chow (1983) is employed to avoid checker-boarding in the velocity and pressure fields. All of the conservation equations in this investigation are solved using a spatial discretization technique of the second order. For this study, a completely implicit first-order approach has been used as the time accuracy to ensure consistency. A variation of Issa's PISO approach (Issa, 1986) is used to solve the transport equations. The variable time step approach is employed in this investigation, with beginning, minimum, and maximum time steps of 1E-07, 1E-08, and 2E-06 s, respectively. The time step is optimized for the fewest amount of CFLs, which may be anywhere from one to five. To maintain stability and, if possible, speed up the time step, a method based on variable time steps is employed. Local cell sizes, velocity, speed of sound, and diffusivity inform the Courant-Friedrichs-Lewy (CFL) quantities that set the time step. FSI events can be rigid-body or beam-bending. These events work like open and closed events. Instead of periods, rigid or beam FSI events can be described by translation lengths or rotation degrees. FSI events supersede standard events in conflicts. Events activate or deactivate disconnect triangles, which govern flow between areas. open events deactivate disconnect triangles to enable passage between specified areas. Disconnect triangles prevent flow across areas after a close event. Disconnect triangles trigger symmetry border conditions. CONVERGE does not change the time step to align events with time-steps. CONVERGE conducts events from each time step at the conclusion. After an incident, the time-step will be lowered by ten to better replicate the domain's shock by shutting or linking areas. The RNG k-ε turbulence model of Yahkot (Yakhot and Orszag, 1986) is used to simulate turbulence using the default values for the model parameters. In the typical k-epsilon model, eddy viscosity is derived from a single turbulence length scale; hence, the predicted turbulent diffusion happens only at the stated scale, although in actuality, all scales of motion contribute to turbulent diffusion. The RNG method, a mathematical technique that may be used to develop a turbulence model comparable to the k-epsilon, yields a modified form of the epsilon equation that seeks to account for the different scales of motion by modifying the production term. All these terms are replaced with those of the RNG k-ε turbulence model.

Message Passing Interface (MPI) is used for all parallel simulations. Karypis's (Karypis and Kumar, 1998) nontrivial automated domain decomposition methodology is used here for load-balancing control. The spatial distribution of cells may be very irregular if the computational volume evolves (for instance, if borders are moved) or if cells are added via Automatic Mesh Refinement (AMR).

This work employs the Cartesian cut-cell approach developed by Senecal et al. (2007). A triangulated surface representing the computational domain's volume serves as the starting point for the model. An orthogonal basis grid of size selected by the user is used to fill the volume. The cells of the base grid are separated into polyhedral with arbitrary side lengths, as illustrated in Fig. 4, at the spots where the triangulated surface crosses over into the base grid. For any given size of the base grid, the volume represented by the cut cells will be the same as the volume of the original triangulated surface. Due to the fully automated nature of the mesh generation process, even the most intricate boundary forms and motions may be accommodated with little to no input from the user. The use of regular orthogonal grids is the source of this method's computational friendliness as well as its robust numerical stability. To solve these conservation equations, the finite-volume technique is used since it is the most appropriate method. We have amassed all of the model's values by the time we have reached the middle of the computational cells.

During the working progressions, the flow of the operating fluid in the hermetic reciprocating compressor is turbulent, which is one of the results of pulsation. In this paper, the RNG k-ε turbulence model is used to simulate fluid flow, which has been extensively preferred in the literature. Following are the transport equations for turbulence energy and dissipation rate (Senecal et al., 2007):

$$\frac{\partial}{\partial t}(\rho k)+\frac{\partial}{\partial x_i}(\rho k u_i)=\frac{\partial}{\partial x_j}\left[\left(\mu+\frac{\mu_t}{\sigma_k}\right)\frac{\partial k}{\partial x_j}\right]+P_k-\rho\varepsilon \tag{5}$$

$$\frac{\partial}{\partial t}(\rho \varepsilon)+\frac{\partial}{\partial x_i}(\rho \varepsilon u_i)=\frac{\partial}{\partial x_j}\left[\left(\mu+\frac{\mu_\varepsilon}{\sigma_\varepsilon}\right)\frac{\partial \varepsilon}{\partial x_j}\right]+C_{1\varepsilon}\frac{\varepsilon}{k}P_k-C_{2\varepsilon}^{*}\rho\frac{\varepsilon^2}{k} \tag{6}$$

$$C_{2\varepsilon}^{*}=C_{2\varepsilon}+\frac{C_\mu\eta^3\left(1-\frac{\eta}{\eta_0}\right)}{1+\beta\eta^3} \tag{7}$$

$$\eta=\frac{Sk}{\varepsilon} \tag{8}$$

$$S=\sqrt{(2S_{ij}S_{ij})} \tag{9}$$

where μ_t is the turbulent viscosity. C_μ, σ_k, σ_ε, $C_{\varepsilon1}$, $C_{\varepsilon2}$, η_0 and β are the model constants. Blending the relevant constants from the conventional k-ε model is used to get these values. The following values are the two models' constants: $C_\mu = 0.0845$, $\sigma_k = 0.7194$, $\sigma_\varepsilon = 0.7194$, $C_{\varepsilon1} = 1.42$, $C_{\varepsilon2} = 1.68$, $\eta_0 = 4.38$, $\beta = 0.012$.

Since the four steps that make up one compression cycle of a reciprocating compressor, namely compression, discharge, expansion, and suction, are divided by the opening and closing of the valve, the opening, and closing of the reed valve is the key to numerical simulations for a complete working process of the reciprocating compressor. This is because the four steps that makeup one compression cycle are compression, discharge, expansion, and suction. In this particular piece of research, the opening and closing of the valve are managed by the use of opening/closing event boundary conditions. The state of the applied opening/closing event boundary is what determines whether or not the two fluid domains are linked to one another. The applied opening/closing event boundary is an interface between the two fluid domains. These boundary conditions are implemented between the suction area and the cylinder region, as well as between the cylinder region and the discharge region.

The magnitude of the event surface served as the determining factor in this FSI model in determining the condition of the opening/closing distance boundary. Take the suction valve as an example; when the size of the opening/closing distance is greater than the set value of opening, the flow field of the suction plenum connected with the flow field of the cylinder, and fluid flowed through the interface. This occurred when the size of the opening/closing distance is greater than the set value of the opening. When the size of the opening/closing distance is less than the set value of closing, the surface of the opening/closing distance is considered to be a wall boundary, which partitioned the two fluid fields. This occurred when the size of the opening/closing distance is less than the set value of closing. The opening/closing distance boundary that controls the opening and shutting of the discharge valve is established in the same manner as the boundary that controls the opening and closing of the suction valve.

The opening/closing distance surface area is fixed to 1E-04 m for the suction valve and 2E-06 m for the discharge valve. The flow field on both sides of the valve may not be detached in time if the value is too small, resulting in excessive backflow. If the closure value is set too high, the flow field on both sides of the valve will be severed prematurely, preventing the simulation of the actual flow condition.

3.2. Structure domain

As shown in Fig. 3, the structural domain of the compressor model includes the suction valve, the discharge valve, and the retainer with the discharge valve.

Since the valve plate is assumed to be a rigid model with a single degree of freedom, the ring plate's behavior may be characterized as a rotational motion, and the valve's dynamics can be expressed as follows.

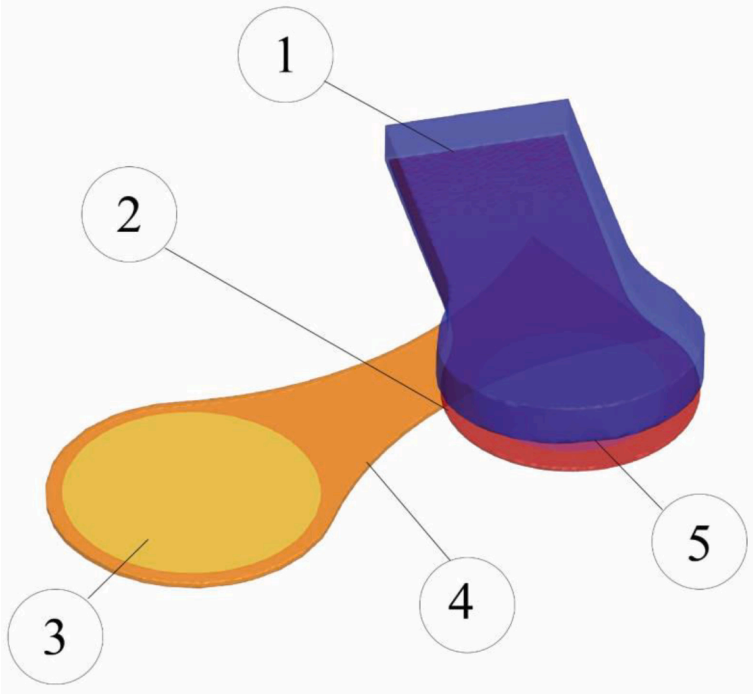


Fig. 3. Structure of solid reed valves. (1) lift limiter, (2) discharge valve, (3) Suction reed valve surface adjacent to the suction port, (4) suction reed valve, (5) Discharge reed valve surface adjacent to the discharge port.

$$M\ddot{x} + C\dot{x} + Kx = F_P + F_O \tag{10}$$

where M is the constant mass matrix, C is the constant damping matrix, and K is the constant stiffness matrix. F is the nodal force vector corresponding to the element stresses. $\dot{x}$ represents nodal point velocity and, $\ddot{x}$ represents nodal point accelerations. x is the vector of incremental nodal point displacement. In the suggested model, a contact condition between the reed valve and the valve seat is added. The reed valve material used in this investigation is HiFlex material.

Conditions of contact are established to simulate the impacts between valve assemblies. Three contact groups are defined in the model, as depicted in Fig. 3: Contact Group 1 between the lift limiter and the discharge reed valve and Contact Group 2 between the discharge reed valve surface adjacent to the discharge port, Contact Group 3 between the suction reed valve surface adjacent to the suction port.

3.3. Fluid-solid interaction modeling

To solve the FSI model, the CFD solver used a technique called the finite volume method to analyze the fluid domain, while the structural solver used a method called the finite element method to investigate the solid domain. Both of these analyses are performed on the FSI model. After that, the FSI solver that is applied in the coupled solution of the two domains is carried out based on the theory.

In the FSI model of the compressor, the coupling of the reed valve with the flow field is realized by three fluid-structure interfaces. These fluid-structure interfaces are the fluid-structure boundary of the discharge reed valve, the fluid-structure boundary of the suction reed, and the fluid-structure boundary of elastic damping. Both the fluid domain and the structural domain are used in the process of delineating the fluid-structure boundaries. The shape of the fluid-structure boundary in the fluid field is made compatible with that in the structure field. This is done so that the two fields would be able to interact.

3.4. Grid independent study

To complete the mesh-independent verification, the outcomes of the simulation are compared after being run with a variety of various mesh sizes. The findings are summarized in Table 4 below. It is discovered that the results of the simulations run with a grid number mesh of 1.5 mm are not significantly different from those runs with a grid number mesh of 1.5 mm. This led us to believe that grid-independent findings may be accomplished with a mesh size of 1.5 mm. As a result, simulations are run using a mesh with a resolution of 1.5 mm .

4. Result and discussion

To verify the accuracy of the FSI model, the findings of the simulations regarding the pV diagram and the lift of the suction valve are compared with the results of the experiments.

4.1. A comparison of the pV diagram with experimental results

Results of numerically and experimentally obtained pV indicator diagrams of the hermetic reciprocating compressor are given in Fig. 4. The rotational speed of the compressor is set to 2100, 1300, and 1600

Table 4
Grid independency results.

	Base mesh size [mm]	Minimum AMR Cells [-]	Minimum AMR Cells [-]	Mass flow rate [g/s]	Compressor work [W]
Grid-1	2	1	10,000	0.38	53.89
Grid-2	2	10,000	50,000	0.38	53.8
Grid-3	2	50,000	75,000	0.375	53.6
Grid-4	2	75,000	100,000	0.371	53.4
Grid-5	2	100,000	200,000	0.369	53.35
Grid-6	1.5	200,000	250,000	0.369	53.19

rpm, and the compressor operates under ASHRAE, domestic refrigerator-specific operating settings such as (25 °C/-20 °C) and (40 °C/-25 °C), respectively, to determine the generating mechanism of pressure pulsation. During the process of simulation, the fluid pressure as well as the lifts of the suction and discharge valves are monitored.

It is discovered through simulation of the operating process of the compressor that the pulsation in the suction space is strictly associated with the movement of the reed valve. This is one of the observations that is made. When the suction reed valve is opened, the refrigerant that is contained within the suction region is injected into the cylinder via the suction plenum. This causes the fluid in the cylinder to move at a much different velocity than before. Because of the difference in velocity of the fluid, the cylinder experiences turbulence as a result of the intensification of the vortices and oscillations that are generated by the difference in velocity. When the discharge reed valve is opened, the refrigerant in the cylinder is inserted into the discharge region through the port. This causes the fluid in the discharge chamber to move at a significantly different velocity than the fluid in the cylinder. Turbulence is caused in the discharge chamber as a result of the difference in the velocities of the fluids presents there. According to the procedure described above, the most significant contributor to the discharge pressure pulsation is the non-uniform change in the fluid.

Fig. 4 also shows a comparison of the simulated and experimental pV diagrams, indicating that the FSI model's calculation of the pressure change in the cylinder is in good agreement with the measured values. The absence of the compressor's suction and discharge pipes from the numerical model may explain the time discrepancy between the experiment and the analysis. A large suction muffler reduces the effect of pressure pulsation on the compressor's ability to draw in isobutane. It should be noted that Pham et al. (2018) investigated a three-dimensional CFD model of a scroll compressor employing circling scrolls and deforming reed valves using CONVERGE software's FSI analysis. They obtained similar pV loop area matching numerical data with experiments.

The area between the condensation pressure and the pV curve in the indication diagram in Fig. 4 indicates the discharge line losses, whereas the area between the evaporation pressure and the pV curve represents the suction line losses. Discharge line losses include discharge port and discharge manifold losses, whereas suction line losses include the suction muffler and suction manifold losses. The suction and discharge line losses are computed using the trapezoidal method and Eq. (11) to determine the specified areas. By calculating these areas, the suction line losses for ASHRAE, (25 °C/-20 °C) and (40 °C/-25 °C) operating conditions are calculated to be 1.90 W, 1.34 W, and 1.81 W, while the discharge line losses are calculated to be 1.26 W, 1.33 W, and 0.75 W for the same operating conditions, respectively.

$$\oint pdV = \sum_{j=1}^{n} \left(\frac{Pc_j + Pc_{j-1}}{2} \right) \left(V_{j-1} + V_j \right) \tag{11}$$

The compression work done by the experiment and the simulation of the compression is compared under three different conditions, as shown in Table 5. The highest inaccuracy that may occur is 2.4%. This demonstrates that the FSI model can be relied upon to accurately mimic the whole of the compression process. In another research that looked at the performance of compressors, Tao et al. (2018), Hopfgartner et al. (2017), Wu et al. (2022), and Rowinski and Dawis (Rowinski et al., 2018) numerically produced compressor work with high convergence, which supported the conclusions that are found in this study about

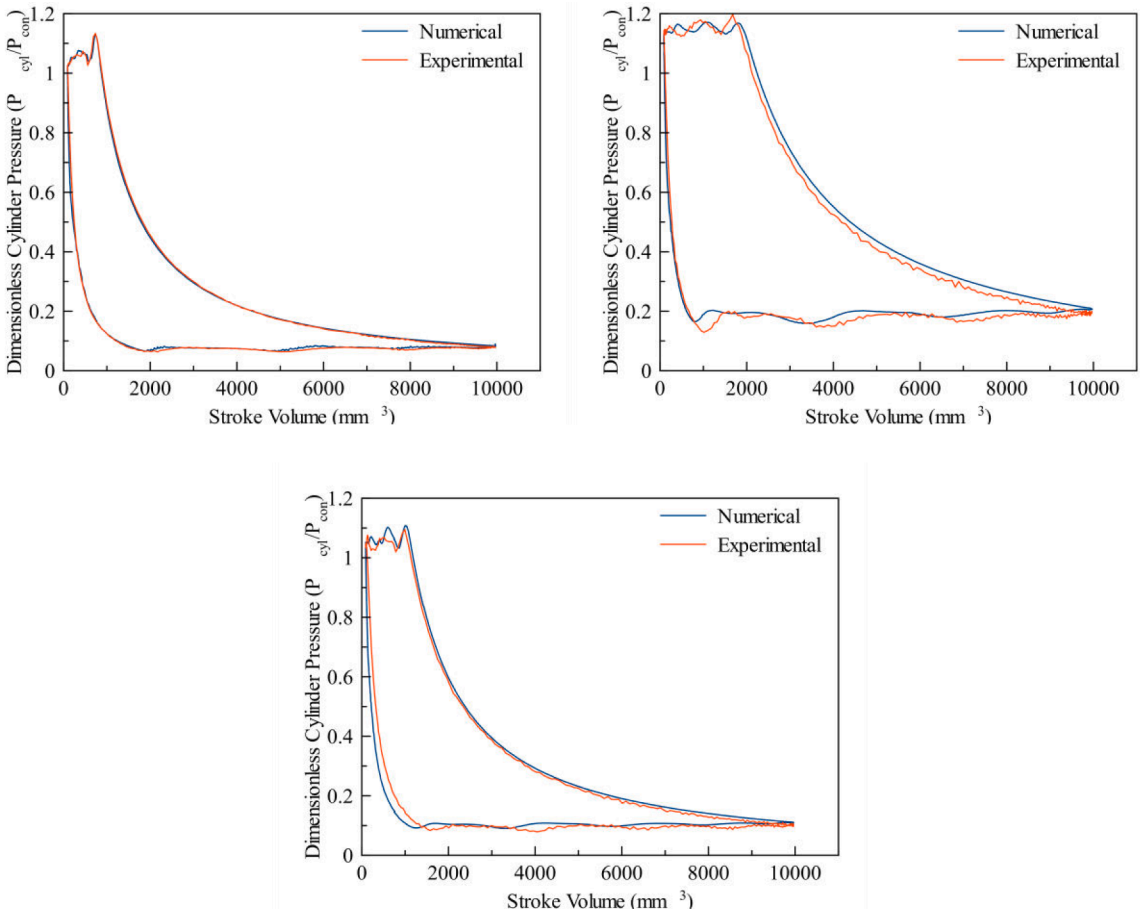


Fig. 4. pV indication diagrams of the investigated hermetic reciprocating compressor under ASHRAE (54.4 °C/-23.3 °C) 2100 rpm and specific refrigerator operating condition (25 °C/-20 °C) 1300 rpm and (40 °C/-25 °C) 1600 rpm respectively.

Table 5
Validation results of compressor work and inner mass flow rate.

Operating condition	Speed	Numerical		Experimental		Differences in compressor work	Difference of mass flow rate
		Compressor work	Mass flow rate	Compressor work	Mass flow rate		
	rpm	W	g/s	%	g/s	%	%
ASHRAE (54.4 °C/-23.3 °C)	2100	52.99	0.360	52.09	0.355	1.79	-1.28
(25 °C/-20 °C)	1300	26.43	0.321	26.59	0.319	-0.6	0.6
(40 °C/-25 °C)	1600	33.79	0.282	34.97	0.289	3.4	2.4

compressor work.

4.2. Numerical and experimental valve oscillation results

The computation that the FSI model uses to depict the motion of the suction reed valve is checked for accuracy using the experimental data. Fig. 5 presents a comparison of the simulated and experimental data for the lift of the suction valve during the suction stage. These results may be found in the text that follows the figure. It has been shown that the imprecision of the theoretical calculation made using the proposed model is not unacceptable. The viscosity of the oil in the compressor is not taken into consideration by the simulation, which is the source of the discrepancy between the estimated result and the experimental results. The researcher Tao et al. (2018) looked at the motion of the suction valve in a reciprocating compressor and used a technique called FSI. Their findings, which reveal similar tendencies and yield equivalent conclusions to those found in the present study, are summarized.

As seen in Fig. 5, the number of times the suction reed valve opens and shuts changes based on the compressor's operating state and speed. There are approximative numbers for the opening/closing distance of the suction reed valve. The opening/closing number and distance of the suction reed valve rely on characteristics like the reed valve's modulus of elasticity, density, thickness, and stiffness, as well as the thermo-physical properties of the gas conditioned in the compressor.

When compared to the discharge reed valve, the effect of low pressure and other viscous and inertial forces acting on the suction reed valve provides a higher convergence to the experimental results. The view presented in this study is supported by the studies conducted by Wu et al. (2022), Zhao et al. (2018), and Hopfgartner et al. (2017) in the literature. The discharge lift limiter, which is depicted as component number 1 in Fig. 3, protects the reed valve from breaking as a result of plastic deformation brought on by excessive valve opening caused by high condensation pressure. In other words, it reduces the discharge valve's opening distance to prevent damage. The suction reed valve does

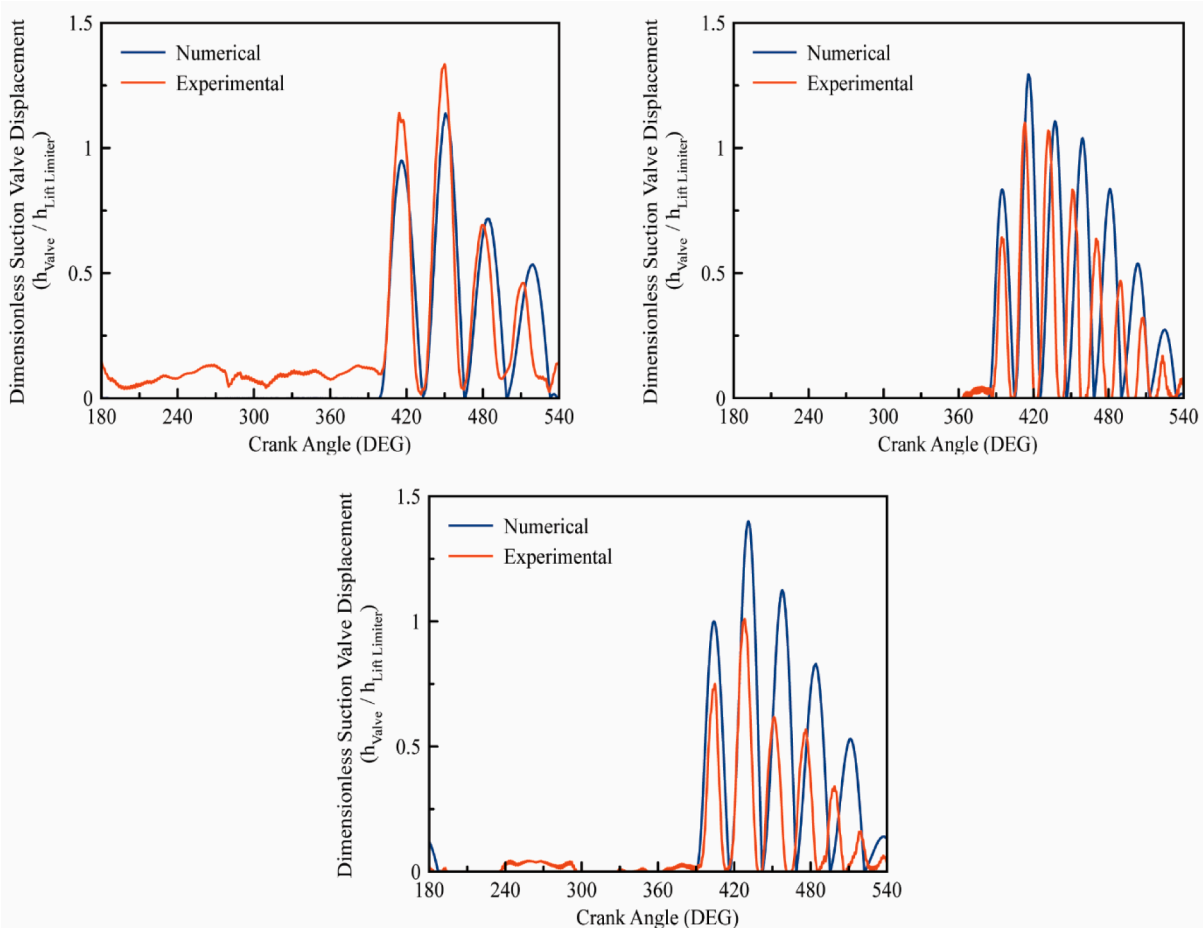


Fig. 5. Predicted suction valve lift and the experimental result of the hermetic reciprocating compressor under ASHRAE (54.4 °C/-23.3 °C) 2100 rpm and specific refrigerator operating condition (25 °C/-20 °C) 1300 rpm and (40 °C/-25 °C) 1600 rpm respectively.

not include the apparatus called this lift limiter. Consequently, the amplitude of the opening of the suction reed valve is greater than that of the discharge reed valve. Since the lift limiter height in this study is 1.05 mm, the maximum opening of the discharge reed valve is 1.05 mm, while the opening amplitude of the suction reed valve can be greater.

Fig. 5 demonstrates that despite the various pressure ratios, the flutter number of the suction reed valve fell as predicted as the compressor speed increased. Depending on the speed of the compressor, the interaction between the refrigerant gas forces and the inertia of the reed valve can explain this phenomenon. While the validation trials utilizing the FSI approach yielded comparable results in terms of trend, the amplitude of each leaf flutter movement varies. This scenario can be described by the sensitivity of the strain-gage measuring instrument used in experimental research, and the sensitivity of the numerical model. While the suction reed valve displacement value is numerically greater for the ASHRAE operating condition than the experimental investigation, the other operating circumstances have lower values. As the mass and stiffness damping coefficient of the reed valve, as well as gas leaks between the reed valve and seating surfaces, are not accounted for in numerical analyses, it is common for them to diverge from experimental results. It should be noted that Rowinski et al. (2018) have also obtained higher experimental results than numerical ones regarding the calculation of displacement of suction valve according to ASHRAE operating condition.

The FSI model's predictions for the motion of the discharge reed valve are also validated by comparing them to experimental data. Fig. 6 shows a comparison between the simulated value and the experimental result for the lift of the discharge valve during the discharge stage. This comparison can be seen in the upper right-hand corner of the figure. It has been proven that the proposed model results in theoretical calculations with an accuracy that is deemed acceptable. During the simulation, if the viscous force of the oil in the compressor is not taken into consideration, there will be a difference between the estimated result and the real data. This disparity might be seen as an error. Tao et al. (2018) have examined the suction valve motion of the reciprocating compressor using the FSI method, showed similar trends, and obtained comparable results with those in the current study.

Fig. 6 depicts how the discharge reed valve opens and shuts in response to the compressor's status and speed. The distance between the opening and shutting of the discharge reed valve is approximate. The discharge reed valve's opening/closing number and distance are determined by its modulus of elasticity, density, thickness, and stiffness, as well as the thermophysical characteristics of the compressor.

Fig. 6 also demonstrates that, as a direct consequence of the phase difference, the discharge reed valve deflected far more than the suction reed valve. This may be seen as a direct simulation of the high pressure and inertial forces present in the exhaust zone, as well as the viscous forces created by the oil used for mechanical lubrication on the reed valve. By the obtained results of the current study, Tao et al. (2018) indicated that the error between the calculation result and the experimental data resulted from the viscous force of oil in the compressor, which is ignored in the simulation.

4.3. Oscillations of the suction and discharge valves

In Fig. 7, the variation of suction and discharge reed valve movement and cylinder gas mass as a function of crank angle for one cycle is depicted. The mass in the cylinder is used to compute the mass flow rate

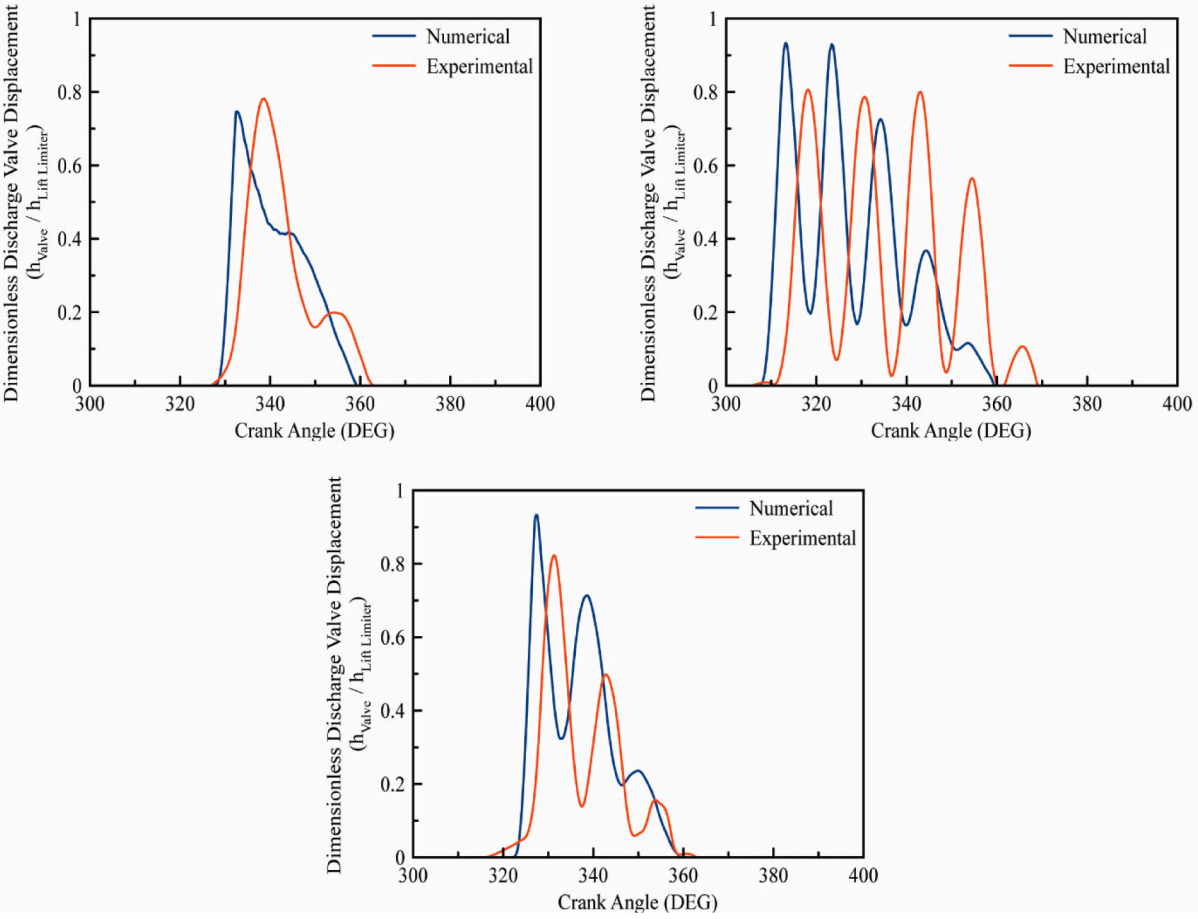


Fig. 6. Predicted discharge valve lift and the experimental result of the hermetic reciprocating compressor under ASHRAE (54.4 °C/−23.3 °C) 2100 rpm and specific refrigerator operating condition (25 °C/−20 °C) 1300 rpm and (40 °C/−25 °C) 1600 rpm respectively.

of the compressor. To determine the net refrigerant mass, the difference between the gas masses in the cylinder before the discharge valve is opened and before the suction valve is opened is subtracted. The mass flow is calculated by dividing the resulting net refrigerant mass by one compressor cycle time. This calculation in the compressor is designed to prevent an error caused by reverse flows to or from the cylinder volume during the suction and discharge valve openings. When the piston is at or near TDC, for ASHRAE (25 °C/-20 °C) and (40 °C/-25 °C) operating conditions, the discharge valve opens at crank angles of 330°, 310°, and 325°, respectively. The pressure difference between the cylinder and the discharge plenum determines the opening of the discharge reed valve; if the cylinder pressure is greater than the discharge plenum pressure, the discharge reed valve opens. As shown in Fig. 7, when the discharge valve opens, the mass of R600a in the cylinder flows into the discharge manifold, causing the R600a mass in the cylinder to decrease. At or near BDC, the suction valve opens at a crank angle of 400° for ASHRAE condition and 390° for both (25 °C/-20 °C) and (40 °C/-25 °C) operating conditions. The pressure difference between the cylinder and the suction manifold determines the opening of the suction reed valve; if the cylinder pressure is lower than the suction manifold pressure, the suction reed valve opens. As shown in Fig. 7, when the suction valve opens, the mass of R600a flows from the suction manifold to the cylinder, increasing the cylinder's volume.

In the majority of hermetic reciprocating compressors, self-extraction reed valves are utilized. In other words, the valve opens and closes automatically in response to the pressure difference between the cylinder and manifold areas. In a hermetic reciprocating compressor, the suction reed valve should open when the piston is at the bottom dead point and the exhaust reed valve should open when the piston is at the top dead center. However, due to the pressure difference, the suction and exhaust reed valves open earlier than these ideal times. Therefore, there is a small change in the crank angle between the discharge valve's closing and the suction valve's opening time. There is a maximum inaccuracy of 3.4% when comparing the mass flow rate of the experimental compression to the simulation of the same compression, which is illustrated in Table 5 and Fig. 7 under three different conditions. This demonstrates that the FSI model can be relied upon to accurately mimic the whole of the compression process. When calculating the operational mass flow rate of a compressor, one needs to take into account the mass that is present in the cylinder region just before the opening of the discharge and suction valves for a cycle. This is shown in Fig. 7, and this mass flow rate must be taken into consideration. It should be noted that Rowinski et al. (2018) investigated the deforming reed valves of a small displacement refrigeration compressor having R-404a and R-449a. They benefited from CONVERGE software's FSI analysis and achieved quite low discrepancies between experimental and numerical data.

In the majority of hermetic reciprocating compressors, self-acting reed valves are utilized as shown in Fig. 3. In other words, the valve opens and closes automatically in response to the pressure difference between the cylinder and manifold areas. In a hermetic reciprocating compressor, the suction reed valve should open when the piston is at the bottom dead point and the exhaust reed valve should open when the piston is at the top dead center. However, due to the pressure difference, the suction and exhaust reed valves open earlier than these ideal times. Therefore, there is a small change in the crank angle between the discharge valve's closing and the suction valve's opening time.

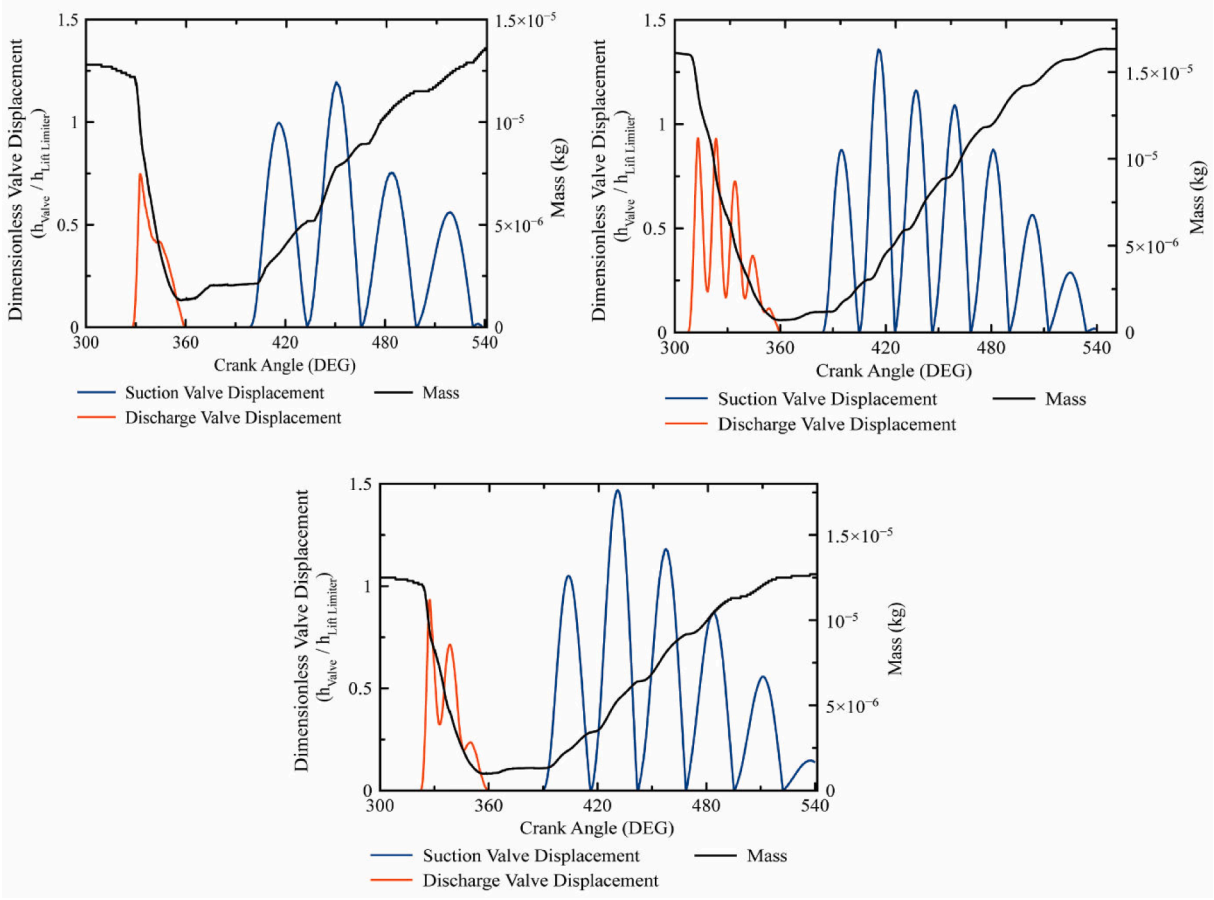


Fig. 7. Predicted mass flow rate result of the hermetic reciprocating compressor under ASHRAE (54.4 °C/-23.3 °C) 2100 rpm and specific refrigerator operating condition (25 °C/-20 °C) 1300 rpm and (40 °C/-25 °C) 1600 rpm respectively.

5. Conclusion

This study validated a model of a hermetic reciprocating compressor using an advanced mesh refinement method at three different operating conditions under ASHRAE (54.4 °C/-23.3 °C) at 2100 rpm and 25 °C/-20 °C at 1300 rpm and 40 °C/-25 °C at 1600 rpm. This method is computationally straightforward and has excellent numerical stability. Using this method as the third one in the literature, the mesh structure of complex geometries is generated without additional time or effort. Thus, the development of the model and the solution takes significantly less time than with other methods. Calculations of the compression process, including the reciprocating compressor reed valve, are performed using CONVERGE. In this work, an FSI approach is presented to investigate the thermodynamic process as well as the motion of the valves in the hermetic reciprocating compressor. Different from the others, no prior study has explored the whole compression cycle, including all four essential phases by showing the compressor's pV and valve oscillation diagrams under these operating conditions. According to the findings of the numerical model, pressure fluctuations within the cylinder should be expected as reliable, and the results have been summed up as follows:

a The FSI model is capable of simulating the opening and shutting of the reed valves in the hermetic reciprocating compressor, which is the essential step in simulating the whole compression cycle of a refrigerator compressor.
b The suggested mesh mapping approach in conjunction with the AMR methodology has been employed effectively to model the transient flow within the compressor and has been able to forecast the thermodynamic performance with good accuracy.
c Unlike the conventional one-dimensional thermodynamic model in the literature, the FSI model allowed for the investigation of both the delayed closing of the suction and discharge valves and the backflow through them. This brought about an advantage for the FSI model.
d In this study, the FSI model is developed, and the mechanism of pressure pulsation generation is investigated. Because of the pressure difference, the reed valve is forced to open, which allows fluid to go from an area of high pressure to an area of low pressure. This inhomogeneous shift in the fluid inside the cavity is the major source of pressure pulsation. The variation in velocity causes oscillation and turbulence in the fluid within the cavity.
e Depending on the evaporation pressure, condensation pressure, and compressor speed parameters, this source of pulsation in the compressor exhibits varying characteristics and effects, and directly influences the number of opening and closing on the suction and discharge reed valves, as well as its amplitude and width.
f The components of the compressor, such as the lift limiter and discharge valve, in the exhaust line, make it more difficult to model than the suction line. In FSI studies, gas leaks from the discharge valve occur during the expansion process after the exhaust process at high pressure; thus, it is required to examine the grid structure of the discharge valve and restraint components with more elements and adopt the appropriate sealing measures.
g Pulsative flow is the most influential irreversibility on compressor performance. Examining the discharge phase of the indicator diagram indicated which pressure wave in the suction and discharge lines is an overshoot and which is a flutter. These flow parameters discovered are evidence of pulsative flow in the compressor.
h Produced refrigerator compressors should exhibit great performance under a variety of operating conditions based on varying climatic situations. Consequently, performance testing and FSI analyses must be assessed based on various operating situations. The fact that it shows varied properties under different operating situations and even at the same compressor speed, as demonstrated by the derived curves, is the most significant factor in this case.
i Numerically obtained results demonstrate a significant degree of convergence between experimental and numerical ones in this investigation. To achieve convergence, a study of independence from network structure, time step, and the number of cycles are necessary. In addition to them, as few CFLs as feasible should be used. In this study, the number of CFLs varies dynamically, and a maximum of two dynamic meshes are used. In addition, the numerical solution is near to the experimental results due to the low convergence criteria of the software.

Declaration of Competing Interest

The authors declare that they have no known competing financial interests or personal relationships that could have appeared to influence the work reported in this paper.

Acknowledgement

The authors would like to thank Arcelik A.Ş. for their support during the experimental research. This study is based on the Ph.D. dissertation completed at Yıldız Technical University. Convergent Science provided CONVERGE licenses and technical support for this work.

Supplementary materials

Supplementary material associated with this article can be found, in the online version, at doi:10.1016/j.ijrefrig.2023.01.028.

References

Chae, H.M., Kim, C.N., 2010. A numerical study with FSI mode on the characteristics of pressure fluctuation and discharge valve motion in rotary compressors with single and dual muffler. Int. J. Precis. Eng. Manuf. 11 (4), 589–596.
Choi, Y.S., Lee, J.H., Jeong, W.B., Kim, I.G., 2010. Dynamic behavior of valve system in linear compressor based on fluid-structure interaction. J. Mech. Sci. Technol. 24 (7), 1371–1377.
Coskun, U.C., Gunes, H., Sarioglu, K., 2016. A numerical model of fluid structure interaction of a fluttering valve. In: Proceedings of the 5th International Conference on Jets, Wakes and Separated Flows (ICJWSF2015). Springer, Cham, pp. 421–429.
Dhar, S., Ding, H., & Lacerda, J. (2016). A 3-D transient CFD model of a reciprocating piston compressor with dynamic port flip valves.
González, I., Naseri, A., Rigola, J., Pérez-Segarra, C.D., Oliva, A., 2017. A fluid-structure interaction solver for the fluid flow through reed type valves. In: IOP Conference Series: Materials Science and Engineering, 232. IOP Publishing, 012032.
González, I., Naseri, A., Rigola, J., Pérez-Segarra, C.D., Oliva, A., 2019. Detailed prediction of fluid-solid coupled phenomena of turbulent flow through reed valves. In: IOP Conference Series: Materials Science and Engineering, 604. IOP Publishing, 012064.
He, Z., Jian, Z., Wang, T., Li, D., Peng, X., 2017. Investigation on the variation of pressure in the cylinder of the refrigerator compressor based on FSI model. IOP Conference Series: Materials Science and Engineering, 232. IOP Publishing, p. 012005.
Hopfgartner, J., Posch, S., Zuber, B., Almbauer, R., Krischan, K., Stangl, S., 2017. Reduction of the suction losses through reed valves in hermetic reciprocating compressors using a magnet coil. In: IOP conference series: materials science and engineering, 232. IOP Publishing, 012034.
Hwang, I.S., Park, S.J., Oh, W., Lee, Y.L., 2017. Linear compressor discharge valve behavior using a rigid body valve model and a FSI valve model. Int. J. Refrig. 82, 509–519.
Issa, R.I., 1986. Solution of the implicitly discretised fluid flow equations by operator-splitting. J. Comput. Phys. 62 (1), 40–65.
Jin, H., Sun, Z., Gu, J., Huang, Y., Wang, X., Zhang, Q., Shen, X., 2020. A detrending-extracting-zooming-based speed measurement method for hermetic reciprocating compressor. Measurement 157, 107654.
Karypis, G., Kumar, V., 1998. A Software Package For Partitioning Unstructured graphs, Partitioning meshes, and Computing Fill-Reducing Orderings of Sparse Matrices. University of Minnesota, Department of Computer Science and Engineering, Army HPC Research Center, Minneapolis, MN, p. 38.
Kawabata, S., Deguchi, R., Matsuura, H., 2022. Calculation of internal flow in a compressor with valve motion. In: Proceedings of the International Compressor Engineering Conference at Purdue.
Kim, J., Wang, S., Park, S., Ryu, K., & La, J. (2006). Valve dynamic analysis of a hermetic reciprocating compressor.
Lang, W., Almbauer, R., Berger, E., & Nagy, D. (2010). Comparative study of two different equations of state for modelling a reciprocating compressor for the refrigerant R600a.
Lang, W., Almbauer, R., Jajcevic, D., 2010a. Usage and validation of a fluid structure interaction methodology for the study of different suction valve parameters of a hermetic reciprocating compressor. Int. J. Multiphys. 4 (1), 65–82.

Park, S.J., Hwang, I.S., Oh, W.S., Lee, Y.L., 2017. A study on cycle performance variation of a linear compressor considering valve behavior. J. Mech. Sci. Technol. 31 (9), 4481–4488.

Pham, H.D., Brandt, T., & Rowinski, D.H. (2018). Modeling a scroll compressor using a cartesian cut-cell based CFD methodology with automatic adaptive meshing.

Redlich, O., Kwong, J.N., 1949. On the thermodynamics of solutions. V. An equation of state. Fugacities of gaseous solutions. Chem. Rev. 44 (1), 233–244.

Rhie, C.M., Chow, W.L., 1983. Numerical study of the turbulent flow past an airfoil with trailing edge separation. AIAA J. 21 (11), 1525–1532.

Rowinski, D.H., & Davis, K.E. (2016). Modeling reciprocating compressors using a Cartesian cut-cell method with automatic mesh generation.

Rowinski, D.H., Sadique, J., Oliveira, S.J.D., & Real, M. (2018). Modeling a reciprocating compressor using a two-way coupled fluid and solid solver with automatic grid generation and adaptive mesh refinement.

Senecal, P.K., Richards, K.J., Pomraning, E., Yang, T., Dai, M.Z., McDavid, R.M., ... & Shethaji, T. (2007). A new parallel cut-cell Cartesian CFD code for rapid grid generation applied to in-cylinder diesel engine simulations (No. 2007-01-0159). SAE Technical Paper.

Tan, Q., Pan, S.L., Feng, Q.K., Yu, X.L., Wang, Z.L., 2015. Fluid–structure interaction model of dynamic behavior of the discharge valve in a rotary compressor. Proc. Inst. Mech. Eng. Part E J. Process Mech. Eng. 229 (4), 280–289.

Tao, W., Guo, Y., He, Z., Peng, X., 2018. Investigation on the delayed closure of the suction valve in the refrigerator compressor by FSI modeling. Int. J. Refrig. 91, 111–121.

... & Wu, W., Guo, T., Peng, C., Li, X., Li, X., Zhang, Z., He, Z., 2022. FSI simulation of the suction valve on the piston for reciprocating compressors. Int. J. Refrig. 137, 14–21.

Yakhot, V., Orszag, S.A., 1986. Renormalization group analysis of turbulence. I. Basic theory. J. Sci. Comput. 1 (1), 3–51.

Zhao, B., Jia, X., Sun, S., Wen, J., Peng, X., 2018. FSI model of valve motion and pressure pulsation for investigating thermodynamic process and internal flow inside a reciprocating compressor. Appl. Therm. Eng. 131, 998–1007.